Constructing Robust Liquid State Machines to Process Highly Variable Data Streams

Stefan Schliebs[1], Maurizio Fiasché[2], and Nikola Kasabov[1]

[1] Knowledge Engineering and Discovery Research Institute
Auckland University of Technology, New Zealand
{sschlieb,nkasabov}@aut.ac.nz
[2] Department of Mathematics "F. Brioschi",
Polytechnic Institute of Milan,
Milan, Italy
maurizio.fiasche@ieee.org

Abstract. In this paper, we propose a mechanism to effectively control the overall neural activity in the reservoir of a Liquid State Machine (LSM) in order to achieve both a high sensitivity of the reservoir to weak stimuli as well as an improved resistance to over-stimulation for strong inputs. The idea is to employ a mechanism that dynamically changes the firing threshold of a neuron in dependence of its spike activity. We experimentally demonstrate that reservoirs employing this neural model significantly increase their separation capabilities. We also investigate the role of dynamic and static synapses in this context. The obtained results may be very valuable for LSM based real-world application in which the input signal is often highly variable causing problems of either too little or too much network activity.

Keywords: Liquid State Machine, Spiking Neural Networks, Reservoir Computing.

1 Introduction

Liquid State Machines (LSM) [7] employ concepts of the reservoir computing (RC) paradigm [12] and have received lots of attention recently; see [11] for a review. LSM represent an elegant way to exploit the computational capabilities of recurrent SNN without the need to directly train the network itself [5]. Especially interesting is the fact that the reservoir approach appears very suitable to process spatio-temporal data [4] allowing the method to address many challenging real-world problems.

Many studies have demonstrated a competitive performance of the reservoir computing paradigm compared to more traditional techniques [11]. However, it is challenging to configure the reservoir for a particular application [6] due to the large variety of parameter choices such as network topology, neural and synaptic models, input encoding, readout design and learning algorithms. The stability of the reservoir when stimulated by highly variable real world data can also become

A.E.P. Villa et al. (Eds.): ICANN 2012, Part I, LNCS 7552, pp. 604–611, 2012.

an issue [4], since some input samples may consist of only very few spikes, while other samples show a much larger spike activity, i.e. the strength of the stimulus can differ significantly between inputs. The two extremes of too weak and too strong reservoir responses are well known in literature and have been referred to as over-stratification and pathological synchrony, respectively [9,10].

In this paper, we propose to use a dynamic firing threshold model in order to achieve both a high sensitivity of the reservoir to weak stimuli as well as an improved resistance to over-stimulation for strong stimuli. The idea is to employ a mechanism that dynamically changes the firing threshold of a neuron in dependence of its spike activity. A strong stimulation of the neuron results in an increase of its firing rate which will in turn increase the firing threshold. By increasing this threshold, however, the firing rate of the neuron effectively decreases and therefore a dynamic firing threshold can act as a natural control mechanism for the output spike rate of a neuron.

Controlling the spike rate of each neuron allows the reservoir to control its overall neural activity dynamically in dependence of the input stimulus. Our hypothesis is that such a control mechanism also affects the separation capabilities of the reservoir and therefore increases its classification performance in applications. The idea of considering connectionist devices based mainly on the threshold modification is not new per se (see for instance [1]), but the concept was not investigated in the context of LSM, yet. We investigate our hypothesis experimentally by measuring and comparing the separation abilities of a static and a dynamic firing threshold model. Additionally, we investigate the role of a dynamic synaptic model, i.e. short-term synaptic plasticity (STP) [8], in the context of variable input stimuli. In the next section we present the neural, synaptic and threshold model along with the generation of the reservoir followed by the experimental analysis and a discussion of obtained results.

2 Neural and Synaptic Model

In this study, we employ the Leaky Integrate-and-Fire neuron which is arguably one of the best known models for simulating SNN. This neural model is based on the idea of an electrical circuit containing a capacitor with capacitance C and a resistor with a resistance R, where both C and R are assumed to be constant. The dynamics of a neuron i are then described by the following differential equations:

$$\tau_m \frac{\partial V_i}{\partial t} = -V_i(t) + R\ I_i^{\text{syn}}(t) \tag{1}$$

$$\tau_s \frac{\partial I_i^{\text{syn}}}{\partial t} = -I_i^{\text{syn}}(t) \tag{2}$$

The constant $\tau_m = RC$ is called the membrane time constant of the neuron. Whenever the membrane potential V_i crosses a threshold ϑ_i from below, the neuron fires a spike and its potential is reset to a reset potential V_r. We use an exponential synaptic current I_i^{syn} for a neuron i modeled by Eq. 2 with τ_s being a synaptic time constant.

Similar to [2], we define a dynamic firing threshold as a separate differential equation:

$$\tau_\vartheta \frac{\partial \vartheta_i}{\partial t} = \theta - \vartheta_i(t) \tag{3}$$

where θ is the minimum firing threshold of the neuron and τ_ϑ is the time constant for the dynamic threshold. Whenever the neuron i emits a spike, its threshold ϑ_i is increased by a constant $\Delta\theta_i$, i.e. $\vartheta_i \leftarrow \vartheta_i + \Delta\theta_i$.

We investigate both a static and dynamic synapse model in this paper. In the static model, each spike emitted from a pre-synaptic neuron j to a post-synaptic neuron i triggers an update of the synaptic current I_i^{syn}:

$$I_i^{\text{syn}} \leftarrow I_i^{\text{syn}} + w_{ji} \tag{4}$$

where $w_{ji} \in \mathbb{R}$ represents the synaptic weight of the connection between neurons j and i. The dynamic synapse model is based on STP proposed by Markram et al. [8] and is modeled using the differential equations:

$$\tau_D \frac{\partial x_i}{\partial t} = 1 - x_i \tag{5}$$

$$\tau_F \frac{\partial u_i}{\partial t} = U_i - u_i \tag{6}$$

where parameters τ_D and τ_F represent time constants for synaptic depression and synaptic facilitation, respectively, and U_i is utilization of synaptic efficacy. In this model, each pre-synaptic spike travelling from a pre-synaptic neuron j to neuron i triggers:

$$I_i^{\text{syn}} \leftarrow I_i^{\text{syn}} + w_{ji}\ x_i\ u_i \tag{7}$$

$$u_i \leftarrow u_i + U_i(1 - u_i) \tag{8}$$

$$x_i \leftarrow x_i(1 - u_i) \tag{9}$$

We note that the order of these equations is important for the simulation of the model. The sign of weight w_{ji} models either inhibitory or excitatory synapses.

The described neural and synaptic models are experimentally investigated using the following four different combinations:

Model A – static synapses and static firing thresholds, i.e. $\Delta\theta_i = 0$;
Model B – dynamic synapses and static firing thresholds;
Model C – static synapses and dynamic firing thresholds;
Model D – dynamics synapses and dynamic firing thresholds.

The aim of this study is to determine which reservoir employing one of these four models reports the best separation capabilities.

2.1 Reservoir

We construct a reservoir having a small-world inter-connectivity pattern as described in [7]. A recurrent SNN is generated by aligning 200 neurons in a

three-dimensional grid of size $4 \times 5 \times 10$. In this grid, two neurons A and B are connected with a connection probability

$$P(A, B) = C \times e^{\frac{-d(A,B)}{\lambda^2}} \tag{10}$$

where $d(A, B)$ denotes the Euclidean distance between two neurons and λ corresponds to the density of connections which was set to $\lambda = 3$ in all simulations. Parameter C depends on the type of the neurons. We discriminate into excitatory (ex) and inhibitory (inh) neural types resulting in the following parameters for C: $C_{ex-ex} = 0.3$, $C_{ex-inh} = 0.2$, $C_{inh-ex} = 0.5$ and $C_{inh-inh} = 0.1$. The network contained 80% excitatory and 20% inhibitory neurons.

We define the 4×5 neurons located in the first layer of the grid as the input neurons. These neurons are stimulated by the input spike trains as described in the next section. The spiking activity of all neurons in the reservoir occurring in a time window of 10ms is recorded and referred to as the liquid state of the reservoir. More specifically, the liquid state at time t is a binary vector indicating whether a certain neuron has fired or not in the time window $[t, t + 10\text{ms}]$.

In this study, we restrict ourselves to explore a single reservoir only and leave the optimization of the liquid for future directions. In other words, we keep the topology of the network along with its connection weight matrix constant for all the experiments.

3 Experiments

This study investigates the hypothesis whether a dynamic firing threshold can improve the separation capabilities of reservoirs in the context of highly variable input stimuli. The idea is to construct four different reservoirs, each employing one of the four neural models defined in the previous section. Then these four reservoirs are stimulated by inputs of varying strength. We model the stimulus strength by controlling the spike frequency of the input neurons. The higher the frequency, the stronger the input stimulus injected into the reservoir.

For this purpose, we construct a simple synthetic data set. We generate ten uniformly distributed random input spike patterns each consisting of 4×5 individual spike trains. We ensure that the spike trains of pattern i, $0 \leq i \leq 9$ exhibit a specific spike frequency $F_i \in \{2, 4, 8, \ldots, 140\}$Hz.

We consider each of the ten input stimuli as a class pattern. From each pattern, we generate five copies which were jittered using a Gaussian distribution with a standard deviation of 1msec. Therefore, our data set is balanced and contains a total of 50 samples distributed over ten classes. Figure 1 shows one sample of each class of the data set.

3.1 Separation Metric

For comparing the separation properties of reservoirs, we adopt an interesting metric that was recently introduced by Norton et al. [10]. For this procedure

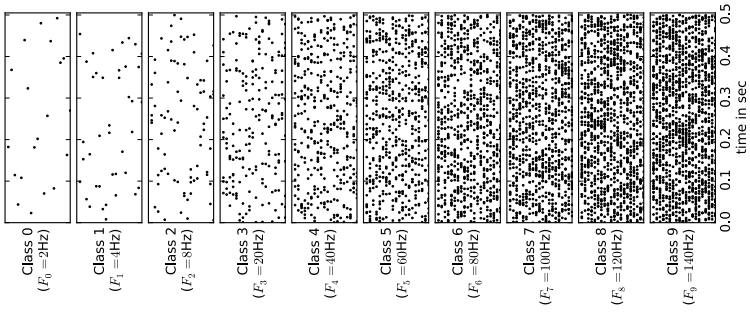

Fig. 1. Synthetic data set in which the strength of the input stimulus is controlled by the spike rate of the input neurons

the responses of a reservoir to input stimuli are recorded. Each input stimulus is labelled and belongs to one of n classes. The recorded liquid states O are divided into subsets O_l, one subset for each class. The idea of the separation metric is to determine the ratio between the inter-class distance c_d and the intra-class variance c_v. The inter-class distance is defined as:

$$c_d = \sum_{l=1}^{n} \sum_{m=1}^{n} \frac{\|\mu(O_l) - \mu(O_m)\|_2}{n^2} \tag{11}$$

where $\mu(O_l)$ is the center of mass for each class l given by $\mu(O_l) = \frac{\sum_{\mathbf{o} \in O_l} \mathbf{o}}{|O_l|}$ The notation $|\cdot|$ is used for set cardinality and $\|\cdot\|_k$ corresponds to the L_k-norm.

The intra-class variance $c_v = \frac{1}{n} \sum_{l=1}^{n} \rho(O_l)$ is defined as the mean variance of a set of state vectors O_l with $\rho(O_l)$ being defined as

$$\rho(O_l) = \frac{\sum_{\mathbf{o} \in O_l} \|\mu(O_l) - \mathbf{o}\|_2}{n} \tag{12}$$

The separation of a liquid Ψ that produces the response $O = \{O_l | l = 1, \ldots, n\}$ is then defined as

$$\mathrm{Sep}_{\Psi}(O) = \frac{c_d}{c_v + 1} \tag{13}$$

We refer to [10] for a more detailed discussion of the separation metric.

For most practical applications, the ability of the reservoir to discriminate between weak and strong inputs is not difficult. However, the classification task becomes more challenging for inputs belonging to different classes but exhibiting similar stimulus strengths. Therefore, we are primarily interested in the separation of neighboring classes, i.e. the separation between samples of class i and samples of class $i + 1$ for $0 \leq i < 9$.

3.2 Results

Preliminary experiments were undertaken to determine the most suitable parameter configurations for each of the four reservoirs. More specifically, we varied the

firing threshold ϑ, the threshold increase $\Delta\theta$, the threshold time constant τ_θ, the time constant of synaptic depression τ_D and the utilization parameter U in order to determine which combination reported the highest average separation. In total 487 different configurations were examined resulting in the following parametrization:

Model A – ϑ=7mV, $\Delta\theta$=0
Model B – ϑ=1mV, $\Delta\theta$=0, τ_D=400ms, τ_F=1ms, U=0.1
Model C – ϑ=4mV, $\Delta\theta$=7.5mV, τ_θ=50ms
Model D – ϑ=0.5mV, $\Delta\theta$=5mV, τ_θ=50ms, τ_D=400ms, τ_F=1ms, U=0.1

All other parameters were kept identical for each of the four constructed reservoirs: membrane time constant τ=30msec, synaptic time constant τ_s=5msec, reset potential V_r=0V, refractory period of 1msec, membrane resistance R=1MΩ. The sparse connection weight matrix of the reservoir was randomly initialized in the interval $[0, 12]$mV. We simulated the reservoir for 1sec of biological time in which the network received the prepared spike trains of our data set during the first 500msec. For the experiments, we used our own LSM toolkit based on the simulator Brain [3].

Figure 2a presents the reservoir responses for the four tested models. Each diagram shows a typical raster plot of neural activity of all neurons; a black dot indicates a spike of a specific neuron at a specific time. Each column in Figure 2a shows the reservoir responses of a particular model while a row indicates the class of the stimulus that was used to produce this response.

The reservoir employing a static threshold and a static synaptic model (Model A) is insensitive to the weakest stimulus (class 0) and even to the stronger inputs of class 2. Clearly, for these inputs the reservoir suffers from over-stratification. However, once the stimulus reaches a certain strength (class 3), the neural activity of the reservoir spontaneously increases. For the strongest stimuli (class 9), the response displays effects of pathological synchrony, since the network remained active for $\approx$ 800msec even though its input signal is absent after 500msec of the simulation.

Figure 2c shows the accumulated neural activity[1] of all tested models. We note the dramatic increase of neural activity from class 2 to class 3 stimuli for Model A reservoirs. As expected, the effects of over-stratification and pathological synchrony have a negative impact on the separation capabilities of the reservoir, cf. Figure 2b. The Model A reservoir reported the lowest separation among all test models. Only the separation between class 2 and class 3 stimuli is high due to the spontaneous increase of neural activity for class 3 stimuli.

Reservoirs using either dynamic synapses or dynamic firing thresholds or both (Model B, C, D) are sensitive even to the weakest stimuli in our experiment, cf. 2a. From Figure 2c we observe that also in these reservoirs the neural activity increases for stronger stimuli, however, more smoothly and less spontaneously compared to Model A reservoirs. Clearly, this smoother behavior also has a positive impact on the separation of these reservoirs. The separation is significantly higher in all dynamic reservoirs (Model B, C, D).

[1] Represented by the number of all spikes in the response of the reservoir.

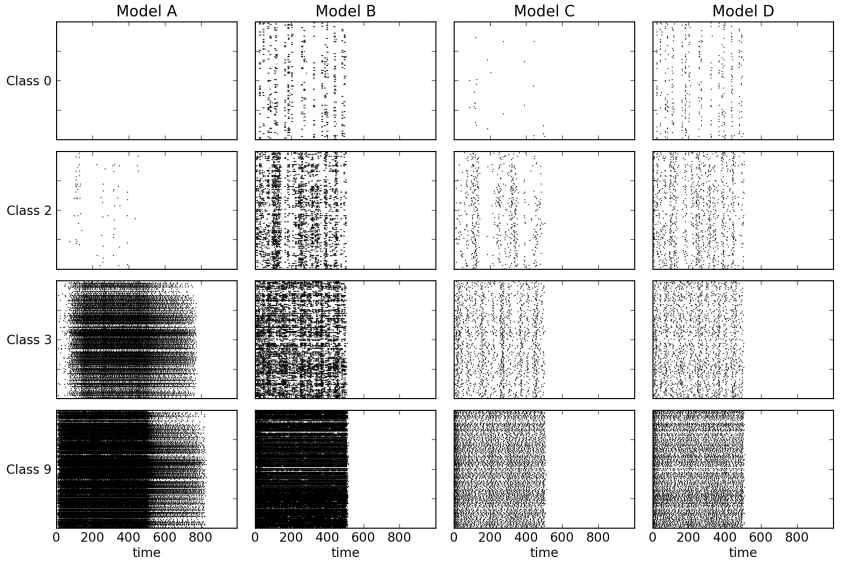

(a) Raster plots of spike activity

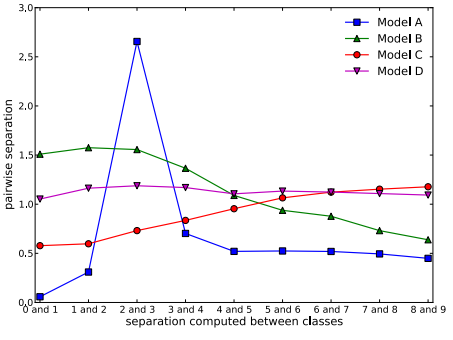

(b) Comparison of separation

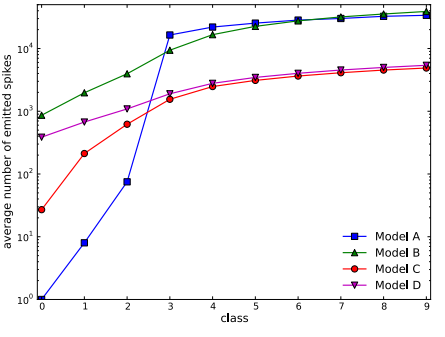

(c) Number of emitted spikes per class

Fig. 2. Simulation results obtained from all four tested models

The most balanced behavior is reported by the reservoirs using both a dynamic synaptic and dynamic firing threshold model, cf. Figure 2b, Model D. With a separation that is almost independent of the stimulus strength, this model appears to combine the good separation characteristics of Model B and Model C. For real-world application, the consistency of this model regarding its separation capability is desired and potentially highly beneficial.

4 Conclusions and Future Directions

In this paper, we have experimentally shown that dynamic firing thresholds in combination with dynamic synapses can significantly improve the separation capabilities of the reservoir independent of the variability of the injected input stimuli. Among the here investigated models, this behavior is the most suitable for future real-world applications. The presented dynamic firing threshold model is computationally inexpensive and an implementation is straightforward. On the other hand, reservoirs with static thresholds and static synapses are prone to the effects of over-stratification and pathological synchrony. Future studies may investigate self-adapting threshold parameters in order to reduce the efforts necessary for identifying suitable LSM configurations.

References

1. Apolloni, B., Bassis, S., Clivio, A., Gaito, S., Malchiodi, D.: Modeling individuals aging within a bacterial population using a pi-calculus paradigm. Natural Computing 6, 33–53 (2007)
2. Gerstner, W., Kistler, W.M.: Spiking Neuron Models: Single Neurons, Populations, Plasticity. Cambridge University Press, Cambridge (2002)
3. Goodman, D., Brette, R.: Brian: A simulator for spiking neural networks in Python. BMC Neuroscience 9(suppl. 1), P92 (2008)
4. Goodman, E., Ventura, D.: Spatiotemporal pattern recognition via liquid state machines. In: International Joint Conference on Neural Networks, Vancouver, BC, pp. 3848–3853 (2006)
5. Kasinski, A.J., Ponulak, F.: Comparison of supervised learning methods for spike time coding in spiking neural networks. Int. J. of Applied Mathematics and Computer Science 16, 101–113 (2006)
6. Lukoševičius, M., Jaeger, H.: Reservoir computing approaches to recurrent neural network training. Computer Science Review 3(3), 127–149 (2009)
7. Maass, W., Natschläger, T., Markram, H.: Real-time computing without stable states: A new framework for neural computation based on perturbations. Neural Computation 14(11), 2531–2560 (2002)
8. Markram, H., Wang, Y., Tsodyks, M.: Differential signaling via the same axon of neocortical pyramidal neurons. Proceedings of the National Academy of Sciences 95(9), 5323–5328 (1998)
9. Norton, D., Ventura, D.: Preparing more effective liquid state machines using Hebbian learning. In: International Joint Conference on Neural Networks, IJCNN 2006, pp. 4243–4248. IEEE, Vancouver (2006)
10. Norton, D., Ventura, D.: Improving liquid state machines through iterative refinement of the reservoir. Neurocomputing 73(16-18), 2893–2904 (2010)
11. Schrauwen, B., Verstraeten, D., Campenhout, J.V.: An overview of reservoir computing: theory, applications and implementations. In: Proceedings of the 15th European Symposium on Artificial Neural Networks, pp. 471–482 (2007)
12. Verstraeten, D., Schrauwen, B., D'Haene, M., Stroobandt, D.: An experimental unification of reservoir computing methods. Neural Networks 20(3), 391–403 (2007)